Insights into a membrane contactor based demonstration unit for CO2 capture

Nieminen Harri, Järvinen Lauri, Ruuskanen Vesa, Laari Arto, Koiranen Tuomas, Ahola Jero

DOI: 10.1016/j.seppur.2019.115951

Insights into a membrane contactor based demonstration unit for CO_2 capture

H. Nieminen*[1], L. Järvinen[2], V. Ruuskanen[2], A. Laari[1], T. Koiranen[1], J. Ahola[2]

1 Lappeenranta-Lahti University of Technology, Laboratory of Process Systems Engineering, P.O. Box 20, FI-53851 Lappeenranta, Finland

2 Lappeenranta-Lahti University of Technology, Laboratory of Control Engineering and Digital Systems, P.O. Box 20, FI-53851 Lappeenranta, Finland

Abstract

A continuously operated CO_2 capture unit, based on absorption in a membrane contactor and low-temperature vacuum desorption, is demonstrated. The major advantage of membrane contactors is their high specific interfacial area per unit volume. The unit is designed to be modular to allow different absorption membrane modules and stripping units to be tested, with the aim of capturing CO_2 from simulated flue gases at concentrations down to the ambient concentration. In addition, desorption can be performed under vacuum to improve the desorption efficiency. The experimental unit incorporates comprehensive measurements and a high level of automation, with heat integration and continuous measurement of electricity consumption providing real-time estimates of the energy consumed in the capture process.

In preliminary tests, the results of which are described herein, a 3M Liqui-Cel™ polypropylene hollow-fiber membrane module and a glass vacuum chamber were used for absorption and desorption, respectively, along with a potassium glycinate amino acid salt absorbent solution. This solution has high surface tension and is fully compatible with the polypropylene membrane unit used. In preliminary tests, the highest observed CO_2 flux was 0.82 mol m^{-2} h^{-1}, with a CO_2 product purity of above 80%. The calculated overall mass transfer coefficient was comparable to reference systems. The performance of the unit in its current setup was found to be limited by the desorption efficiency. Due to the low desorption rates, the measured specific energy consumption was exceedingly high, at 4.6 MJ/mol CO_2 (29.0 MWh/t) and 0.8 MJ/mol CO_2 (5.0 MWh/t) of heat and electricity, respectively. Higher desorption temperatures and lower vacuum pressures enhanced the desorption efficiency and reduced the specific energy consumption. The energy efficiency could be improved via several methods in the future, e.g., by applying ultrasound radiation or by replacing the current vacuum chamber stripping unit with a membrane module or some other type of desorption unit.

Keywords

CO_2 capture, membrane contactor, vacuum, stripping, desorption, amino acid salt, potassium glycinate

Declarations of interest: none

1. Introduction

The development and implementation of carbon capture technologies is vital to mitigate the growing global CO_2 emissions, which have been linked to detrimental climatic effects, most notably global warming [1]. Carbon capture refers to the separation of carbon dioxide (CO_2) from point emission sources, or potentially directly from the atmosphere [2]. In the carbon capture and storage (CCS) approach, the captured CO_2 is stored underground in geological formations like aquifers or depleted oil or gas fields [3]. Alternatively, carbon capture and utilization (CCU) aims to convert the captured CO_2 into valuable products, such as fuels or chemicals [4].

The most established technology for the separation of CO_2 from flue gases or process streams involves the absorption of CO_2 into basic solutions such as aqueous amines, most commonly monoethanolamine (MEA) [5, 6]. In the amine absorption process, CO_2 is chemically absorbed into the solution and then released by heating the CO_2-loaded solution [3]. The significant amount of heat required for the regeneration of the solvent constitutes one of the main costs of any CO_2 capture process [6]. Thus, reducing the energy consumption of CO_2 capture is a major motivation for the development of alternative processes.

One potential method to intensify CO_2 capture is the use of membrane gas-liquid contactors, in which CO_2 is absorbed into the liquid absorbent via mass transfer through a porous, non-selective membrane [7, 8]. Compared to conventional absorption equipment, membrane contactors offer a significant increase in the interfacial area per unit volume [9, 10]. In addition, the interfacial area remains constant regardless of the operating conditions, allowing flexible operation and independent adjustment of the gas and liquid flow rates. The orientation of the module can also be freely selected, and its modular design allows for simple and linear scale-up by increasing the number of modules and total membrane area.

To maximize the interfacial area, membrane gas-liquid contactors are commonly fabricated using hollow fibers [7]. In hollow fiber modules, the membrane fibers are usually packed in parallel bundles inside a shell, with one fluid flowing inside the fibers (lumen-side) and the other outside the fibers (shell-side). However, the added mass transfer resistance caused by the membrane represents a disadvantage. In order to minimize this resistance, microporous polymeric membranes are commonly utilized, with polypropylene (PP) and polytetrafluoroethylene (PTFE) being particularly well studied [8]. The porous membranes are not selective to CO_2; instead, selectivity is facilitated by the chemical absorption of CO_2 into the absorbent solution. The membrane must be hydrophobic in order to resist wetting by the aqueous solution, as the mass transfer is severely limited when the membrane is operated in wetted mode [11]. Selection of the absorbent is also vital in preventing wetting. PP membranes have been found to be incompatible with common amine absorbents for longer contact times due to the low surface tension of the liquid and the chemical changes induced in the membrane surface structure [12, 13, 14].

Due to the wetting of PP membranes, which are more affordable than PTFE membranes, by aqueous amines, the use of alternative absorbents in membrane contactors is of interest. The use of aqueous amino

acid salts has been proposed, as their CO_2 absorption rates and capacities are comparable to those of amine solutions [15] and their high surface tension results in low wetting tendency [16]. In addition, the low volatility and toxicity of amino acid salts compared to amines is advantageous. A variety of amino acid salts have been considered for CO_2 absorption [17, 18]. One example is potassium glycinate [15, 19, 20, 21], which is formed via the neutralization of the amino acid glycine with potassium hydroxide.

The application of a vacuum to lower the solvent regeneration temperature and the corresponding energy consumption has been suggested [22, 23, 24, 25]. Lowering the regeneration temperature would also allow common membrane materials incapable of withstanding high operating temperatures to be utilized. The aim of the present study is to test and analyze the continuous absorption and desorption of CO_2 by a membrane contactor with potassium glycinate as the absorbent. Reports of such continuous processes are relatively scarce, as the majority of the previous literature has focused only on the absorption stage in non-steady-state operation. However, some reports of continuous processes at the laboratory and pilot scale are available [26, 27, 28, 29, 20].

Building on these developments, the present work demonstrates a continuously operated CO_2 capture unit based on absorption in a membrane contactor and low-temperature desorption under an applied vacuum. Here, the amino acid salt potassium glycinate is used as the absorbent, and a commercially available PP hollow fiber module is used as the membrane contactor. The aim of the present paper is to provide an overview of the equipment design, including its measurement and control capabilities, and to present and discuss the initial observations and results obtained using the unit. A more detailed characterization of the CO_2 absorption performance will be the subject of upcoming research.

2. Experimental

2.1. CO_2 capture unit

The continuously operated CO_2 capture unit consists of a hollow fiber membrane module as the absorber, a glass vessel that acts as a stripper, and a buffer tank for the absorbent solution. A flowsheet of the unit is presented in Figure 1. The PP hollow fiber membrane contactor (Liqui-Cel 2.5 x 8 Extra-Flow) was supplied by 3M. The membrane surface area of the module is 1.4 m^2. In the membrane module, the absorbent flows upwards inside the hollow fibers (lumen side, volume 0.15 l), while the inlet gas flows countercurrent on the shell side (volume 0.4 l). The inlet gas consists of a mixture of nitrogen (90% v/v, unless otherwise stated) and CO_2 (10% v/v) for simulated flue gas composition. The gas flows are controlled by mass flow controllers (Bronkhorst EL-FLOW Select, accuracy ±0.5% reading, ±0.1% full scale). The CO_2 concentration of the inlet gas is verified using an IR analyzer (GMP251 probe, ±0.2 % CO_2, and Indigo 201 transmitter, both supplied by Vaisala). The gas pressure is controlled using a back-pressure controller (Bronkhorst EL-PRESS, ±0.1% reading, ±0.5% full scale) located at the membrane gas outlet. The pressure at the gas outlet is maintained 0.1 bar below the liquid inlet pressure in order to avoid wetting of the membrane by the

absorbent solution. The CO_2 concentration of the outlet gas is measured using a separate IR analyzer (Vaisala GMP251 probe and Indigo 201 transmitter).

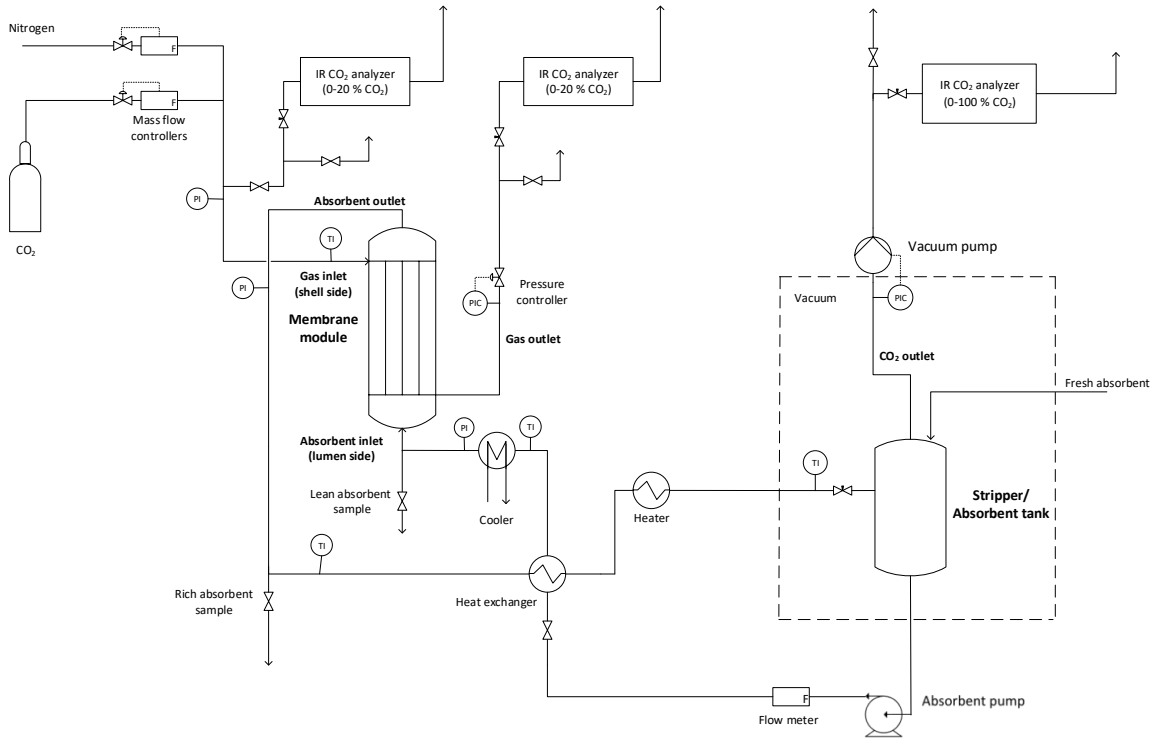

Figure 1 Flowsheet of the experimental CO_2 capture unit.

Liquid is pumped through the system by a magnetic drive gear pump (Pulsafeeder Eclipse E12). The liquid flow rate is measured using a flow meter (Litre Meter LMX.48, ±2% reading) located directly after the pump. The CO_2-lean absorbent pumped at the regeneration temperature (60-80 °C) is first cooled in a plate heat exchanger (Alfa Laval, heat transfer area 1.6 m^2) in which the heat is transferred to the cold absorbent exiting the membrane module. The liquid is then cooled to the absorption temperature (10-30 °C) in another plate heat exchanger (Alfa Laval, heat transfer area 0.2 m^2) with cooling water as the cold fluid. The temperature of the cooling water is controlled via a circulating cooler (Lauda Variocool VC5000, ±0.05 °C). After flowing through the membrane module, the CO_2-rich absorbent is first heated in the heat exchanger and then heated to the regeneration temperature in a hot water heater. The heater consists of an electronic heating element and a coiled absorbent pipe inside a stainless-steel shell. The liquid pressure on the absorption side can be adjusted via a manual needle valve located before the stripper.

In the vacuum regeneration experiments, the gas outlet from the stripper vessel was connected to a vacuum pump (Vacuubrand MZ 2C NT) via an automatic vacuum control unit (Vacuubrand CVC-3000, ±1 mbar, hysteresis 2%). The vacuum pump is equipped with a condenser to condense the solvent and water vapor.

The outlet gas from the vacuum pump is routed to an IR CO_2-analyzer (CO2Meter CM-0052, ±3% reading, ± 0.5% full scale) with a 0-100% v/v measuring range. In addition to CO_2, the analyzer measures the oxygen concentration with a 0-100 % v/v measuring range. **Figure 2** presents a photograph of the unit.

Figure 2 Photograph of the CO_2 capture unit. 1. Membrane contactor, 2. vacuum desorption vessel.

2.2. Measurement and control

The control and data acquisition system is implemented using LabVIEW software. The data acquisition system (NI cDAQ-9189) is used for data gathering and analog control signal output. 4-20 mA analog input signals, measured with a NI 9208 module (accuracy ±0.76% reading), are used for temperature measurements with Pt100 thermistors, pressure measurements, absorbent flow rate measurement, CO_2 analyzers, and mass flow controller feedback signals. A 4-20 mA analog output module (NI 9266, ±0.76 reading, ±1.4% full scale) is used to set the reference values for the mass flow controllers, the back-pressure controller, and the hot water heater. The internal temperature of the hot water heater is controlled via a PI control implemented in LabVIEW, and the 4-20 mA reference signal, which is equal to a power of 0-4.5 kW, is supplied to the REVO S three-phase thyristor power controller.

The analog input signals are sampled with a frequency of 2 kHz, and the mean value of 200 samples is then processed. Therefore, the control and data logging loop is executed with a frequency of 10 Hz. The circulating cooler and the vacuum pump are controlled over an RS232 serial bus with a loop time of around 1 s. The absorbent pump frequency converter is controlled and the electrical power measurement is read via Modbus/TCP with a loop time of roughly 1 s.

The electrical supply power is measured with a Sentron PAC3200 (±0.5% reading) three-phase power analyzer equipped with MAK 62/W 25/1A current transformers. The circulating cooler and hot water heater are excluded from the electrical power measurement. Thus, the heating power of the absorbent is estimated based on the measured flow rate and temperature difference.

2.3. Procedure

The potassium glycinate absorbent was prepared by the neutralization of glycine (Sigma-Aldrich, >99%) with an equimolar amount of potassium hydroxide (Sigma-Aldrich, >85 wt%) in purified water. The solutions were prepared in a glass vessel equipped with a cooling water jacket. The concentrations of all the solutions were verified using potentiometric titration (Mettler-Toledo T50) using 1 M hydrochloric acid, and were within 1% of the nominal concentration. In the CO_2 capture experiments, the feed gas consisted of a mixture of nitrogen (>99.5%) and CO_2 (>99.99%).

The equipment was filled with 6 l of the absorbent solution; using this volume, the liquid level in the absorbent vessel was approximately half the vessel height. The system was started by flowing nitrogen through the membrane contactor, after which the liquid flow was started. The flows of CO_2 and nitrogen were then adjusted to reach the desired gas flow rate and composition. The CO_2 concentration (vol%) of the feed gas was verified by directing a portion of the flow to the IR-analyzer. Following this verification, the flow of feed gas to the analyzer was closed in order to measure the exact flow rate being delivered to the membrane contactor. The heater and cooler (Lauda) were turned on to adjust the liquid temperature during absorption and desorption. The pressure of the liquid entering the membrane module was adjusted using the manual needle valve located before the desorption vessel. In the vacuum desorption runs, the vacuum pump was switched on and the vacuum pressure was controlled by the vacuum control valve.

Unless otherwise stated, all experimental data were collected under steady-state conditions, as indicated by stable operating conditions (temperatures, flow rates, and pressures) together with a stable CO_2 concentration at the outlet of the membrane module (measured using the IR analyzer). The steady-state data were collected for periods of approximately 1 min in the LabView environment, and the final results were calculated as the average values during the sampling period. Liquid samples were also collected under steady-state conditions to analyze the CO_2 loading of the absorbent (mol CO_2 absorbed per mol of potassium glycinate). One rich solvent sample (collected after the membrane module) and one lean solvent sample (collected before the membrane module) were collected, and each sample was analyzed three times by titration with 1 M hydrochloric acid and measuring the volume of the released CO_2. This analysis

was performed using a specifically designed Chittick-apparatus (Soham Scientific). The repeatability of the triplicate measurements was generally within 1.5% (relative standard deviation) with a maximum accepted deviation of 3.0%.

2.4. Calculation of the results

The CO_2 capture efficiency, i.e., the fraction of CO_2 absorbed from the feed gas, was calculated using the expression:

$$\eta = \frac{\dot{n}_{\mathrm{CO_2,in}} - \dot{n}_{\mathrm{CO_2,out}}}{\dot{n}_{\mathrm{CO_2,in}}} \cdot 100\ \% \quad (1)$$

Where η is the capture efficiency (%) and $\dot{n}_{\mathrm{CO_2,in}}$ and $\dot{n}_{\mathrm{CO_2,out}}$ are the molar flows of CO_2 (mol s^{-1}) in the inlet and outlet gas, respectively. The CO_2 molar flux from the gas phase to the liquid phase in the membrane contactor was calculated as:

$$N = \frac{\dot{n}_{\mathrm{CO_2,in}} - \dot{n}_{\mathrm{CO_2,out}}}{A} \quad (2)$$

Where N is the flux (mol m^{-2} s^{-1}) and A is the membrane surface area (m^2) of the module, as specified by the supplier.

The overall mass transfer process in a membrane gas-liquid contactor consists of diffusion of CO_2 from the bulk gas phase to the gas-membrane interface, through the membrane pores to the membrane-liquid interface, and to the bulk liquid followed by chemical and/or physical absorption. The process can be described by the resistance-in-series model using the individual mass transfer coefficients for the gas, liquid, and membrane phases. The overall gas-phase mass transfer coefficient is given by the following expression [30]:

$$\frac{1}{K_{\mathrm{g}}} = \frac{1}{k_{\mathrm{g}}} + \frac{1}{k_{\mathrm{m}}} + \frac{1}{m k_{\mathrm{l}} E} \quad (3)$$

Where k_{g}, k_{m}, and k_{l} are the gas, membrane, and liquid mass transfer coefficients, respectively, m is the distribution coefficient of CO_2 between the gas and liquid phases (Henry's constant in the case of physical absorption), and E is the enhancement factor caused by the chemical reaction, which is defined as the ratio of the absorption flux in the presence of the reaction and the flux with only physical absorption taking place.

To characterize the mass transfer performance of the present system, the gas-side overall mass transfer coefficient was calculated as:

$$K = \frac{N}{\Delta C_{\mathrm{m}}} \quad (4)$$

Where K is the overall mass transfer coefficient (m s^{-1}) and ΔC_m is the logarithmic mean driving force based on the gas-phase concentrations:

$$\Delta C_{\mathrm{m}} = \frac{\left(C_{\mathrm{g,in}} - C^{*}_{\mathrm{g,in}}\right) - \left(C_{\mathrm{g,out}} - C^{*}_{\mathrm{g,out}}\right)}{\ln\left[\left(C_{\mathrm{g,in}} - C^{*}_{\mathrm{g,in}}\right)\left(C_{\mathrm{g,out}} - C^{*}_{\mathrm{g,out}}\right)\right]} \quad (5)$$

Here, $C_{g,in}$ and $C_{g,out}$ out are the measured CO_2 concentrations in the inlet and outlet gas (mol m^{-3}) and $C^{*}_{g,in}$ and $C^{*}_{g,out}$ are the inlet and outlet gas-phase CO_2 concentrations (mol m^{-3}) in equilibrium with the corresponding liquid-phase concentrations. The solubility data of Portugal et al. [31] for CO_2 in 1 M potassium glycinate were utilized to calculate the equilibrium concentrations. The gas-phase concentration was plotted against the liquid-phase concentration in the CO_2 partial pressure range relevant to the present experiments (100-1000 kPa), and an exponential curve was fitted to the data. As a result, the following correlation was found:

$$C^{*}_{\mathrm{g,i}} = 1.4 \cdot 10^{-4} e^{0.014 C_{\mathrm{l,i}}} \quad (6)$$

Where $C_{\mathrm{l,i}}$ is the liquid-phase CO_2 concentration (mol m^{-3}).

The heat duty required for heating the absorbent from the absorption temperature to the desorption temperature was estimated as:

$$Q_{\mathrm{h}} = \rho \dot{V} c_{\mathrm{p}} \Delta T \quad (7)$$

Where Q_{h} is the heat duty (W), $\dot{V}$ is the absorbent volume flow rate (m^3 s^{-1}), ΔT is the temperature difference (°C) between the desorption temperature and the temperature of the pre-heated absorbent leaving the plate heat exchanger, ρ is the absorbent density, approximated by the density of water (1000 kg m^{-3}), and c_{p} is the absorbent heat capacity, which was approximated using the heat capacity of pure water (4186 J kg^{-1} K^{-1}).

The specific heat consumption (J mol^{-1}) per mol of CO_2 captured was then calculated as:

$$e_{\mathrm{h,CO_2}} = \frac{Q_{\mathrm{h}}}{NA} \quad (8)$$

The specific electricity consumption (J mol^{-1}) was similarly calculated as:

$$e_{\mathrm{e,CO_2}} = \frac{Q_e}{NA} \quad (9)$$

Where Q_{e} is the total measured electrical power (W) of the absorbent pump and the vacuum pump.

2.5. Initial observations and challenges

Based on the initial experimental runs discussed here, it is apparent that the CO_2 absorption stage utilizing a membrane contactor can be run continuously with high degree of stability, providing consistent and reliable measurement data. The automatic gas-side pressure control is capable of maintaining the appropriate trans-membrane pressure under the dynamic conditions present during the start-up phase of the capture unit. The temperature of the absorbent solution entering the membrane module is effectively

controlled by the heat exchanger and thermostat. Based on the limited operational time thus far, the PP membrane module appears to be compatible with the amino acid salt solution, and no indication of membrane wetting has been observed. At the start of the experiments, with unloaded absorbent, the mass transfer performance of the membrane contactor is excellent, with nearly 100% of the CO_2 being absorbed (Section 3).

However, from the initial results discussed below, it is clear that the overall CO_2 capture rate under steady-state conditions is limited by the performance of the current simple desorption unit. The glass vessel utilized as the desorber does not feature a distributor for the incoming absorbent and contains no packing to increase the gas/liquid contact area. As a result, the flow pattern of the liquid entering the vessel is not optimal, and the interfacial area is limited.

The desorption temperature is limited by the use of water as the heating medium in the absorbent heater. The temperature is limited to an absolute maximum of 80 °C, and even at that temperature, stable operation during longer periods was periodically disrupted by the overheating of the water bath. Higher temperatures could be achieved by using a different heat transfer fluid. However, operating the desorber at relatively low temperatures is preferred due to potential energy savings and to allow the utilization of low-grade heat or heat pumps, increased absorbent stability, and the possibility of utilizing membrane contactors at the desorption stage. The latter could significantly improve the mass transfer of CO_2 from the solution by increasing the interfacial area.

The rate at which water evaporated from the absorbent depended on the desorption temperature and vacuum pressure, and the vapor escaping the desorption vessel accumulated in the cold trap of the vacuum pump. In order to avoid excessive evaporation of water, the vacuum pressure was limited based on the boiling point of water at the desorption temperature. Operation at boiling conditions might have improved the desorption performance in the experiments due to the increased interfacial area created by the vapor bubbles and the sweeping effect of the vapor, resulting in a decreased partial pressure of CO_2 inside the vessel. Ideally, the condenser should be placed directly on top of the desorption vessel to allow the reflux of water.

3. Results and discussion

This section presents a summary of the preliminary results from the initial runs using the CO_2 capture unit. Figure 3 presents an example of the evolution of the CO_2 concentration at the membrane outlet during start-up. In addition to the concentration, the corresponding CO_2 capture efficiency is also presented in the figure, and the profiles obtained using no vacuum and an 800-mbar vacuum at a desorption temperature of 60 °C are shown. During the first hour of operation, the unloaded absorbent was capable of near-complete absorption of the CO_2 fed to the membrane module, with a capture efficiency of approximately 100%. However, as the absorbed CO_2 was not completely desorbed from the solution, the CO_2 loading continually increased. The increased loading gradually led to a decrease in the CO_2 flux from the feed gas to the

absorbent, and an increasing fraction of the CO_2 in the feed gas passed through the membrane module uncaptured. The steady state was reached when the absorption flux became equal to the flux of CO_2 desorbed from the solution.

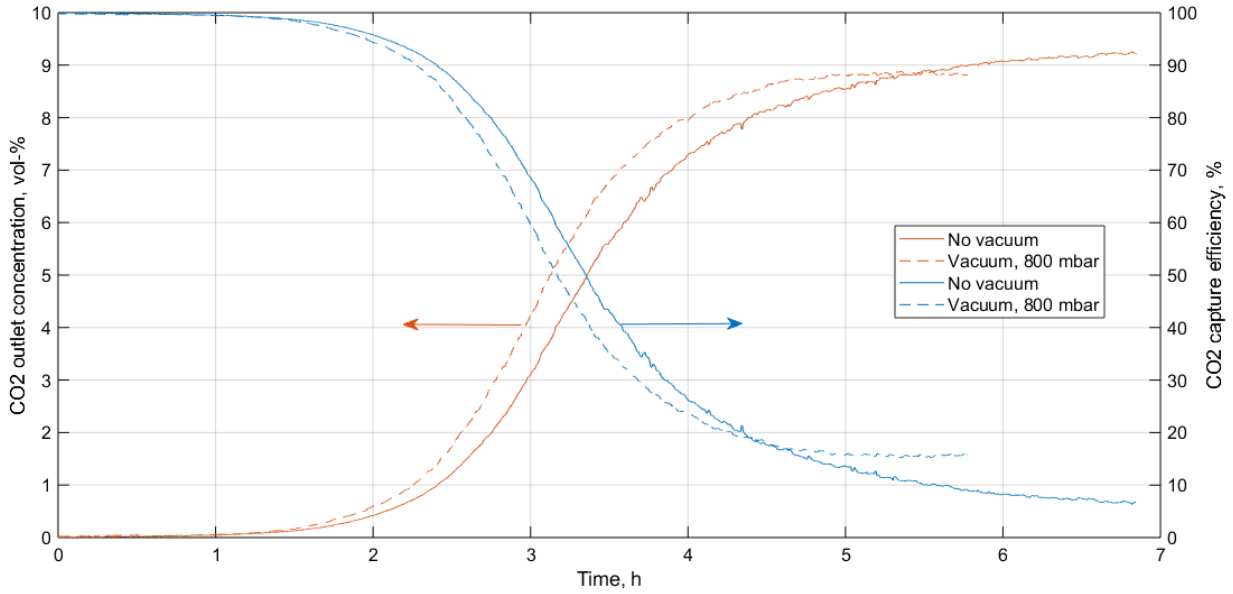

Figure 3 CO_2 concentration and CO_2 capture efficiency during start-up: liquid: 1 l/min (3 M PG), gas: 5 l/min (10% CO_2), absorption: 20 °C, desorption: 60 °C.

When vacuum-assisted desorption was used, the steady state was achieved sooner, and the steady-state CO_2 concentration at the outlet was slightly lower (higher capture efficiency) compared to in desorption without vacuum. This indicates that the vacuum increased the CO_2 flux in the desorption stage. However, even using an 800-mbar vacuum, the desorption rate clearly limited the steady-state absorption performance, with the steady-state CO_2 capture efficiency of approximately 16%, compared to approximately 7% without the vacuum.

Figure 4a presents the effect of the desorption temperature on the CO_2 flux for desorption without vacuum. Clearly, increasing the temperature had a favorable effect on the absorption performance. This can be explained by the more effective desorption of CO_2 from the loaded solution, leading to a lower CO_2 loading in the lean absorbent and increased driving force for absorption. The desorption temperature affects the solubility and resulting equilibrium CO_2 loading of the absorbent, the kinetics of the reactions involved in desorption, and the mass transfer of the desorbed CO_2. However, a detailed discussion of these effects is outside the scope of the present report. In summary, the overall effect of the desorption temperature was drastic in the studied temperature range, with the absorption flux increasing by 460% when the temperature was increased from 60 °C to 80 °C.

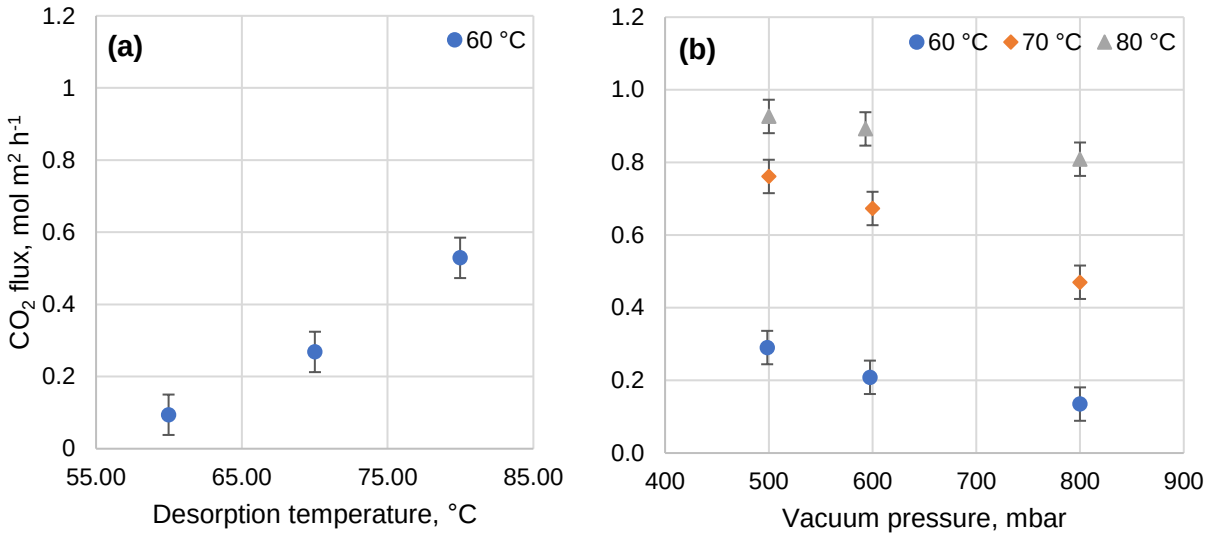

Figure 4 (a) Dependence of the CO_2 absorption flux on the desorption temperature (no vacuum). (b) Dependence of CO_2 absorption flux on the vacuum pressure at desorption temperatures of 60, 70, and 80 °C. Absorbent flow rate: 1 l/min (1 M potassium glycinate), feed gas flow rate: 5 l/min (10 % CO_2), absorption temperature: 20 °C. Error bars correspond to the 95% confidence interval as determined from repeat experiments.

Figure 4b presents the CO_2 flux during desorption under a 800 to 500 mbar vacuum at 60-80 °C. Compared to the non-vacuum results in Figure 4a, the flux generally increased, and decreasing the pressure led to improved performance. The favorable effect of the vacuum can likely be explained by the decreased CO_2 partial pressure in the gas/vapor of the desorption vessel, leading to an increased driving force for desorption. In addition, the vacuum pump continuously swept the desorbed CO_2 out of the vessel, which also increased the driving force. However, the effect of temperature was more pronounced than that of the vacuum pressure. For example, at 60 °C, the flux increased by 115% when the vacuum pressure was lowered from 800 mbar to 500 mbar, while increasing the temperature from 60 °C to 80 °C at 800 mbar of vacuum resulted in a 500% increase in the flux.

Figure 5 presents the overall mass transfer coefficients calculated from Eq. (3) for the different desorption pressures at a temperature of 80 °C. The overall mass transfer coefficient was found to increase with decreasing desorption pressure. This trend was consistent with the variation in the CO_2 flux (Figure 4b) with vacuum pressure, and can be explained by the increased desorption efficiency and the resulting

decrease in the CO_2 loading of the lean absorbent entering the membrane contactor. The lean adsorbent loading varied from 0.48 mol mol^{-1} at 800 mbar to 0.42 mol mol^{-1} at 500 mbar.

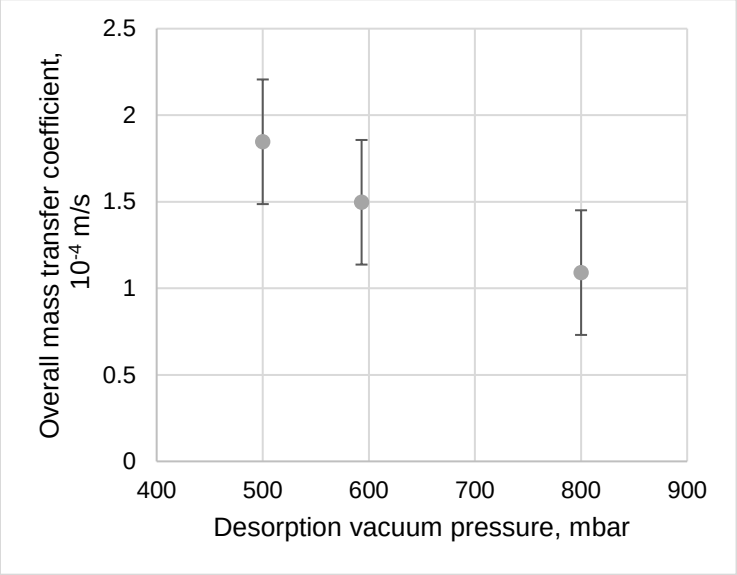

Figure 5 Variation in the gas-side overall mass transfer coefficient with the desorption vacuum pressure at a desorption temperature of 80 °C. Absorbent flow rate: 1 l/min (1 M potassium glycinate), feed gas flow rate: 5 l/min (10 % CO_2), absorption temperature: 20 °C. Error bars correspond to the 95% confidence interval as determined from repeat experiments.

As the driving force for the physical mass transfer from the gas to the liquid was included in the calculation of the overall mass transfer coefficient, the variation in the mass transfer coefficient likely corresponded to variation in the rate of chemical absorption. The higher lean loading under the less-favorable desorption conditions would result in a lower concentration of free amino acid salt in the solution, and a correspondingly lower reaction rate [16]. A similar explanation was given by Lu et al. [32], who also presented data on the overall mass transfer coefficient as a function of the lean solvent loading using N-methyldiethanolamine as the absorbent. Variation in the absorption flux with the CO_2 loading of the lean solution was also reported for various amino acid salt solutions in a screening study by He et al. [33].

The highest overall mass transfer coefficient was 1.9×10^{-4} m s^{-1}. Table I provides a comparison of this value to those in previous reports in the literature; all the listed references employed polypropylene hollow fiber membrane contactors with various absorbents. It should be noted that direct comparison of values determined under very different operating conditions, including different gas and liquid flow rates, temperatures, and solvent type and loadings, should be performed with caution. However, the value found here is well within the range of values found in the literature. Using amino acid salt solutions, Feron and Jansen [26] reported a value one order of magnitude higher utilizing a proprietary solution and custom-built transversal flow membrane module. Lu et al. [21] obtained a value very similar to our result using a potassium glycinate solution. While most of the data were collected using fresh, unloaded solvent, some

329 authors also have also presented results for CO_2-loaded solutions. Compared to these types of results [28,
330 32, 34] the performance of the present system is fairly competitive, especially considering its relatively high
331 lean loading of 0.40 mol mol^{-1}.

332

333 **Table I** Comparison of experimental overall mass transfer coefficients in CO_2 absorption using
334 polypropylene membrane contactors and various absorbents.

Reference	**Absorbent**	**Overall mass transfer coefficient, m s^{-1}**	**Notes**
This work	Potassium glycinate	1.9×10^{-4}	Continuous absorption-desorption, lean loading 0.42
Feron and Jansen, 2002 [26]	CORAL (Proprietary amino acid salt based)	1.6×10^{-3}	Transversal flow module
Mavroudi et al., 2003 [35]	DEA	3.5×10^{-4}	Liqui-Cel module similar to this work
Dindore et al., 2004 [36]	Propylene carbonate	2.0×10^{-5}	Physical absorbent
Kosaraju et al., 2005 [28]	Polyamidoamine dendrimer	2.15×10^{-5}	Continuous absorption-stripping, lean loading not specified
Lu et al., 2005 [32]	MDEA	3.0×10^{-5} 0.8×10^{-5} (lean loading 0.3)	Variation of overall mass transfer coefficient with lean loading presented
Franco et al., 2008 [34]	MEA	4.3×10^{-4}	Simulated regenerated solution with lean loading of 0.27-0.30
Lu et al., 2009 [21]	Potassium glycinate	1.7×10^{-4}	

Lin et al., 2009 [37]	MDEA, AMP	3.3×10^{-4} (AMP) 7.7×10^{-5} (MDEA)	
Chabanon et al., 2011 [12]	MEA	3.3×10^{-4}	Wetting and performance monitored over long operating periods
Wang et al., 2013 [38]	Blended MEA, MDEA	6.8×10^{-4}	
Scholes et al., 2015 [39]	MEA	5.5×10^{-6}	Significant pore wetting observed
Scholes et al., 2015 [40]	BASF PuraTreat (Proprietary amino acid salt based)	7.0×10^{-6}	Pilot plant with real flue gas, significant pore wetting due to pressure fluctuations

The measurement of the CO_2 concentration of the outlet gas leaving the desorption unit allowed evaluation of the selectivity of the absorption process. As the feed gas in the present experiments consisted of only CO_2 and nitrogen, the analysis gave an indication of the CO_2/N_2 selectivity, as dictated by the chemical nature of the absorbent solution. Figure 6 presents the CO_2 concentration of the outlet gas during vacuum desorption at 500-600 mbar and 60-80 °C. The CO_2 concentration ranged from 84 to 95 vol%, and no trends could be observed with respect to the desorption temperature and vacuum pressure. These values corresponded to CO_2/N_2 selectivities of 5 to 20. However, the reliability of these measurements was questionable, as oxygen concentrations of up to 3 vol% were also detected in the outlet gas. As oxygen was not present in the feed gas, the presence of oxygen can only be explained by air remaining in the system or by leaks in the vacuum system. As such, the measured CO_2 concentrations should be considered only as rough estimates, probably giving the lower limit of the actual concentration range.

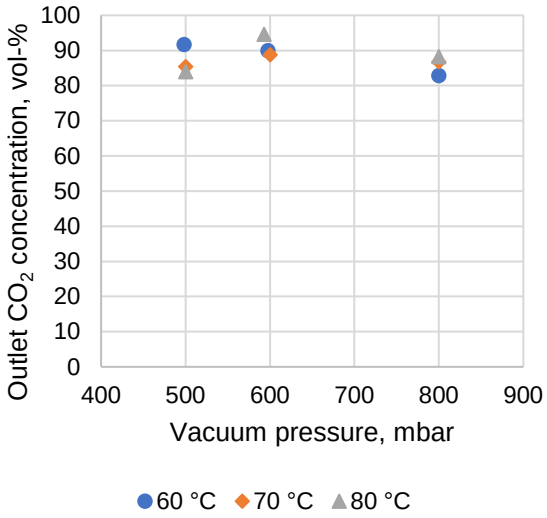

Figure 6 Effect of vacuum pressure and desorption temperature on the CO_2 concentration of the outlet gas leaving the desorber. Absorbent flow rate: 1 l/min (1 M potassium glycinate), feed gas flow rate: 5 l/min (10 % CO_2), absorption temperature: 20 °C.

The energy consumption of the capture unit consists of the heat required to heat the loaded absorbent to the desorption temperature and the electricity consumed by the absorbent and vacuum pumps. Figure 7 presents the specific energy consumption obtained at a desorption temperature of 80 °C under 500-800 mbar vacuum. The electricity consumption was minor compared to the heat required: 4.1 MJ/mol of heat and 0.7 MJ/mol of electricity were consumed during desorption at 500 mbar. These conditions represented the lowest energy consumption among the preliminary runs, as the specific energy consumption was higher when lower desorption temperatures were used. The increased heating requirement at higher temperature was offset by the increased desorption efficiency. For the same reason, lowering the vacuum pressure led to lower heat consumption, while the specific electricity consumption remained essentially constant due to the increased power required by the vacuum pump.

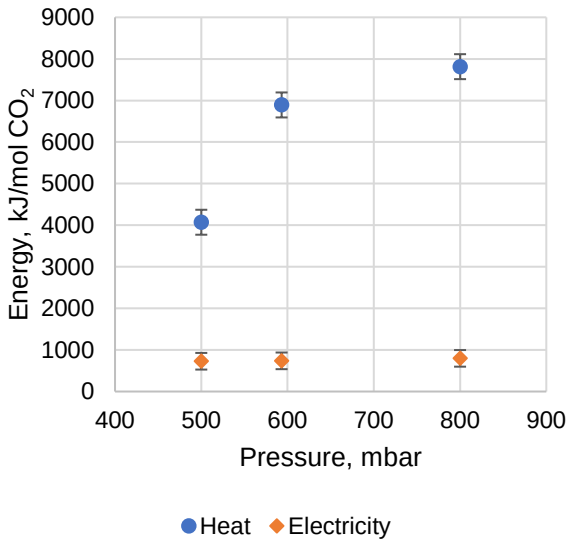

Figure 7 Specific heat and electricity consumption per mole of CO_2 captured during desorption at 80 °C and 500-800 mbar vacuum. Absorbent flow rate: 1 l/min (1 M potassium glycinate), feed gas flow rate: 5 l/min (10% CO_2), absorption temperature: 20 °C.

The data available in the literature for the energy consumption of regeneration using membrane and/or vacuum technology are relatively limited, and the results vary significantly depending on the type of experimental system employed and the method used to estimate the energy consumption. Table II presents a summary of the specific energy consumption values found in the literature. Two types of approaches can be identified in the referenced works. In the first approach, the experiments and calculations are limited to the stripping stage in various configurations, and absorption and solvent circulation are not included [41, 42, 43]. Here, the energy consumption values range from 200 to 780 kJ kg CO_2^{-1}.

In the approach followed in this work, similar to Mulukutka et al. [44], the heat consumption is estimated based on the heating of the solvent in continuous absorption-stripping circulation. The energy consumption found in the current study is closely comparable to that reported by Mulukutka et al. This method seems to lead to energy consumption figures that are at least two orders of magnitude higher than those obtained using the first method. Part of the difference seems to arise from the experimental configuration: limiting the experiments to only the stripping stage allows the optimization of the operating conditions for effective and energy efficient desorption, while the operation in the continuous absorption-stripping mode requires also the consideration of the absorption performance when setting the operating parameters, such as the liquid flow rate. Compared to the work of Wang et al. [43], the liquid flow rate is higher in our case, leading to higher sensible heat requirement for heating the solvent. However, the major difference is the much higher desorption efficiency of the membrane contactor stripping unit demonstrated by Wang et al. [43], indicating the potential for this type of technology.

385 **Table II** Comparison of the specific energy consumption in vacuum- and membrane-based CO_2
386 stripping processes.

Reference	Method	Energy consumption, kJ kg CO_2^{-1}	Notes
This work	Potassium glycinate, 60-80 °C, 50-80 kPa	1.05×10^5 (heat) 1.82×10^4 (electricity)	Includes solvent heating and pumping, vacuum pump
Yan et al., 2009 [41]	MEA, 35 °C, 10-50 kPa	200	Includes vacuum pump but not solvent pumping or heating
Fang et al., 2012 [42]	MEA, PP membrane contactor as stripper, steam sweep, 70 °C, 10-48 kPa	200	Energy consumption increased at lower vacuum due to increased steam generation Solvent pumping and heating not included
Wang et al., 2014 [43]	MEA, PP, and PVFD contactors, 75 °C, 5-80 kPa	780	Includes sensible and latent heat of solvent Higher desorption flux with PVDF but improved stability with PP contactor
Mulukutka et al., 2014 [44]	Ionic liquid absorbent, PP module with fluorosiloxane coating, continuous absorption (50 °C) and stripping (85 °C, 98 kPa)	1.36×10^5	Considers heat of absorption and sensible heat of solvent, but not vacuum pump

387

388 The primary approach for improving the energy efficiency would be to increase the desorption efficiency.
389 Increasing the temperature is not the preferred approach, as operation at relatively low regeneration
390 temperatures is the explicit aim. However, applying lower vacuum pressures and employing intensified
391 mass transfer equipment, including membrane contactors, is another potential approach. The use of
392 membrane contactors in the desorption stage in conjunction with an applied vacuum to increase the driving
393 force and gas sweep could significantly increase the desorption performance. It should be noted that
394 membrane-based desorption is limited to lower regeneration temperatures due to the limited high-

temperature stability of polymeric membranes. Intensification of the desorption stage could also be achieved by means of ultrasound radiation, which will also be explored in a future work.

In addition to modifications to the design of the experimental unit, the energy efficiency could also be improved by optimizing the operating parameters, such as the liquid and gas flow rates and the absorbent type and concentration. As the energy required for heating the solvent is linearly dependent on the liquid flow rate, minimizing the liquid flow rate relative to the gas flow rate would yield significant efficiency benefits. An optimum ratio could likely be found at which the liquid flow rate would be minimized without significant reduction in the CO_2 flux. At the optimum liquid/gas flow ratio, absorption would still be controlled by interphase mass transfer, while further decrease in the liquid flow rate would result the absorption being limited by the chemical reaction due to the depletion of free amino acid salt [16]. Increasing the absorbent concentration should also result in improved efficiency, as a greater concentration of CO_2 could be adsorbed while circulating and heating the same amount of liquid in the system, and accordingly, the CO_2 desorption flux would be higher at the same solvent heating duty.

4. Conclusion

A continuously operated CO_2 capture unit based on absorption in a membrane contactor and low-temperature desorption under an applied vacuum was demonstrated. The purpose of the unit is to capture CO_2 from simulated flue gas and process CO_2 stream concentrations down to ambient concentration. The experimental unit incorporates comprehensive measurements and a high level of automation, with heat integration and continuous measurement of electricity consumption potentially providing realistic estimates of the energy consumed in the capture process.

In preliminary runs using a potassium glycinate absorbent, the steady-state CO_2 absorption performance was found to be limited by the desorption stage. During start-up, the unloaded absorbent could achieve nearly complete absorption of the CO_2 fed to the membrane absorption module; the capture efficiency subsequently decreased as the CO_2 loading of the absorbent increased. Higher desorption temperatures and lower vacuum pressures were found to increase the desorption efficiency, resulting in a higher CO_2 absorption flux. The highest flux of 0.82 mol m^{-2} h^{-1} (corresponding to 36 g CO_2 captured per hour) was found at a desorption temperature of 80 °C under a 500-mbar vacuum. The corresponding overall mass transfer coefficient (1.9×10^{-4} m s^{-1}) was comparable to previously published values for polypropylene contactors with various absorbents.

Increasing the desorption temperature and lowering the vacuum pressure also resulted in decreased specific energy consumption, as the increased heat and electricity consumption were offset by the increased desorption rate. The lowest specific heat and electricity consumption of 4.1 MJ/mol CO_2 (29.0 MWh/t) and 0.7 MJ/mol CO_2 (5.0 MWh/t) were achieved at 80 °C and 500 mbar vacuum. The observed purity of the desorbed CO_2 ranged from 84 to 95 vol%; however, the accuracy of these measurements was potentially compromised by the presence of air in the system.

Based on these initial findings, it is clear that the desorption efficiency of the unit must be improved via modification of the equipment setup and operational conditions. Optimization of the setup and conditions is facilitated by the modular nature of the unit, which allows it to operate with alternative membrane absorption modules and desorption configurations. The use of membrane contactors in the desorption stage could improve the performance via increased interfacial area. Lower vacuum pressures could be attained by eliminating the current operational limitations of the system. At present, the low desorption efficiency leads to very high values for the estimated specific energy consumption. In addition to improvements to the equipment setup, the specific energy consumption could be improved by optimization of the operating parameters, for example, by minimizing the liquid/gas flow ratio and increasing the absorbent concentration.

Nomenclature

A	membrane surface area, m^2
C	concentration, mol m^{-3}
C^*	equilibrium concentration, mol m^{-3}
c_p	heat capacity, J kg^{-1} K^{-1}
E	enhancement factor, -
e	specific energy, J mol^{-1}
K	gas-side overall mass transfer coefficient, m s^{-1}
k	individual mass transfer coefficient, m s^{-1}
N	molar CO_2 flux, mol m^{-2} s^{-1}
$\dot{n}$	molar flow rate, mol s^{-1}
Q	duty, W
T	temperature, K
$\dot{V}$	volumetric flow rate, m^3 s^{-1}
ΔC_m	logarithmic mean driving force, -
η	CO_2 capture efficiency, %
ρ	density, kg m^{-3}

Subscripts

458	e	electricity
459	g	gas
460	h	heat
461	l	liquid
462	in	inlet to the membrane module
463	m	membrane
464	out	outlet from the membrane module

465

466 **5. References**

467

[1] M. Mikkelsen, M. Jørgensen and F. C. Krebs, "The teraton challenge. A review of fixation and transformation of carbon dioxide.," *Energy Environ. Sci.,* vol. 3, p. 43–81, 2010.

[2] J. Wilcox, Carbon Capture, New York: Springer Science+Business Media, LLC, 2012.

[3] M. E. Boot-Handford, J. C. Abanades, E. J. Anthony, M. J. Blunt, S. Brandani, N. Mac Dowell, J. R. Fernández, M.-C. Ferrari, R. Gross, J. P. Hallett, R. S. Haszeldine, P. Heptonstall, A. Lyngfelt, Z. Makuch, E. Mangano and R. T. J. Porter, "Carbon capture and storage update," *Energy Environ. Sci.,* vol. 7, pp. 130-189, 2014.

[4] M. Peters, B. Köhler, W. Kuckshinrichs, W. Leitner, P. Markewitz and T. E. Müller, "Chemical Technologies for Exploiting and Recycling Carbon Dioxide into the Value Chain," *ChemSusChem,* vol. 4, p. 1216 – 1240, 2011.

[5] N. MacDowell, N. Florin, A. Buchard, J. Hallett, A. Galindo, G. Jackson, C. S. Adjiman, C. K. WIlliams, N. Shah and P. Fennell, "An overview of CO_2 capture technologies," *Energy Environ. Sci.,* vol. 3, p. 1645–1669, 2010.

[6] E. S. Rubin, H. Mantripragada, A. Marks, P. Versteeg and J. Kitchin, "The outlook for improved carbon capture technology," *Prog. Energy Combust. Sci.,* vol. 38, pp. 630-671, 2012.

[7] A. Gabelman and S.-T. Hwang, "Hollow fiber membrane contactors," *J. Membr. Sci.,* vol. 159, no. 1-2, pp. 61-106, 1999.

[8] S. Zhao, P. H. M. Feron, L. Deng, E. Favre, E. Chabanon, S. Yan, J. Hou, V. Chen and H. Qi, "Status and progress of membrane contactors in post-combustion carbon capture: A state-of-the-art review of new developments," *J. Membr. Sci.,* vol. 511, pp. 180-206, 2016.

[9] E. Cussler, "Hollow fiber contactors," in *Membrane Processes in Separation and Purification*, Netherlands, Kluwer Academic Publishers, 1994, pp. 375-394.

[10] E. Favre and H. F. Svendsen, "Membrane contactors for intensified post-combustion carbon dioxide capture by gas–liquid absorption processes," *J. Membr. Sci.,* Vols. 407-408, pp. 1-7, 2012.

[11] S. Mosadegh-Sedghi, D. Rodrigue, J. Brisson and M. C. Iliuta, "Wetting phenomenon in membrane contactors – Causes and prevention," *J. Membr. Sci.,* vol. 452, pp. 332-353, 2014.

[12] E. Chabanon, D. Roizard and E. Favre, "Membrane Contactors for Postcombustion Carbon Dioxide Capture: A Comparative Study of Wetting Resistance on Long Time Scales," *Ind. Eng. Chem. Res.,* vol. 50, no. 13, pp. 8237-8244, 2011.

[13] Y. Lv, X. Yu, S.-T. Tu, J. Yan and E. Dahlquist, "Wetting of polypropylene hollow fiber membrane contactors," *J. Membr. Sci.,* vol. 362, no. 1-2, pp. 444-452, 2010.

[14] D. deMontigny, P. Tontiwachwuthikul and A. Chakma, "Using polypropylene and polytetrafluoroethylene membranes in a membrane contactor for CO_2 absorption," *J. Membr. Sci.,* vol. 277, pp. 99-107, 2006.

[15] A. F. Portugal, P. W. J. Derks, G. F. Versteeg, F. D. Magalhães and A. Mendes, "Characterization of potassium glycinate for carbon dioxide absorption purposes," *Chem. Eng. Sci.,* vol. 62, p. 6534 – 6547, 2007.

[16] P. S. Kumar, J. A. Hogendoorn, P. H. M. Feron and G. F. Versteeg, "New absorption liquids for the removal of CO_2 from dilute gas streams using membrane contactors," *Chem. Eng. Sci.,* vol. 57, no. 9, pp. 1639-1651, 2002.

[17] H.-J. Song, S. Park, H. Kim, A. Gaur, J.-W. Park and S.-J. Lee, "Carbon dioxide absorption characteristics of aqueous amino acid salt solutions," *Int. J. Greenhouse Gas Control,* vol. 11, pp. 64-72, 2012.

[18] B. M. S. E. H. &. T. K. Lerche, CO_2 Capture from Flue gas using Amino acid salt solutions., Kgs. Lyngby: Technical University of Denmark (DTU), 2012.

[19] P. S. Kumar, J. A. Hogendoorn and G. F. Versteeg, "Kinetics of the reaction of CO_2 with aqueous potassium salt of taurine and glycine," *AIChE J.,* vol. 49, no. 1, pp. 203-213, 2003.

[20] S. Yan, M.-X. Fang, W.-F. Zhang, S.-Y. Wang, Z.-K. Xu, Z.-Y. Luo and K.-F. Cen, "Experimental study on the separation of CO_2 from flue gas using hollow fiber membrane contactors without wetting," *Fuel Process. Technol.,* vol. 88, pp. 501-511, 2007.

[21] J.-G. Lu, Y.-F. Zheng and M.-D. Cheng, "Membrane contactor for CO_2 absorption applying amino-acid salt solutions," *Desalination,* vol. 249, p. 498–502, 2009.

[22] S. Nii, Y. Iwata, K. Takahashi and H. Takeuchi, "Regeneration of CO_2-loaded carbonate solution by reducing pressure," *J. Chem. Eng. Jpn.,* vol. 28, no. 2, pp. 148-153, 1995.

[23] M. Fang, S. Yan, Z. Luo, M. Ni and K. Cen, "CO_2 chemical absorption by using membrane vacuum regeneration technology," *Energy Procedia,* vol. 1, pp. 815-822, 2009.

[24] Z. Wang, M. Fang, Y. Pan, S. Yan and Z. Luo, "Amine-based absorbents selection for CO_2 membrane vacuum regeneration technology by combined absorption–desorption analysis," *Chem. Eng. Sci.,* vol. 93, pp. 238-249, 2013.

[25] S. Yan, M. Fang, Z. Wang and Z. Luo, "Regeneration performance of CO_2-rich solvents by using membrane vacuum regeneration technology: Relationships between absorbent structure and regeneration efficiency," *Appl. Energy,* vol. 98, pp. 357-367, 2012.

[26] P. Feron and A. Jansen, "CO_2 separation with polyolefin membrane contactors and dedicated absorption liquids: performances and prospects," *Sep. Purif. Technol.,* vol. 27, pp. 231-242, 2002.

[27] O. Falk-Pedersen, M. Grønvold, P. Nøkleby and F. Bjerve, "CO_2 capture with membrane contactors," *Int. J. Green Energy,* vol. 2, p. 157–165, 2005.

[28] P. Kosaraju, A. S. Kovvali, A. Korikov and K. K. Sirkar, "Hollow Fiber Membrane Contactor Based CO_2 Absorption-Stripping Using Novel Solvents and Membranes," *Ind. Eng. Chem. Res.,* vol. 44, pp. 1250-1258, 2005.

[29] S.-H. Yeon, K.-S. Lee, B. Sea, Y.-I. Park and K.-H. Lee, "Application of pilot-scale membrane contactor hybrid system for removal of carbon dioxide from flue gas," *J. Membr. Sci.,* vol. 257, pp. 156-160, 2005.

[30] J.-L. Li and B.-H. Chen, "Review of CO_2 absorption using chemical solvents in hollow fiber membrane contactors," *Sep. Purif. Technol.,* vol. 41, no. 2, pp. 109-122, 2005.

[31] A. F. Portugal, J. M. Souda, F. D. Magalhães and A. Mendes, "Solubility ofcarbon dioxide in aqueous solutions of amino acid salts," *Chem. Eng. Sci.,* vol. 64, pp. 1993-2002, 2009.

[32] J. Lu, L. Wang, X. Sun, J. Li and X. Liu, "Absorption of CO_2 into Aqueous Solutions of Methyldiethanolamine and Activated Methyldiethanolamine from a Gas Mixture in a Hollow Fiber Contactor," *Ind. Eng. Chem. Res.,* vol. 44, pp. 9230-9238, 2005.

[33] F. He, T. Wang, M. Fang, Z. Wang, H. Yu and Q. Ma, "Screening Test of Amino Acid Salts for CO_2 Absorption at Flue Gas Temperature in a Membrane Contactor," *Energy Fuels,* vol. 31, p. 770−777, 2017.

[34] J. Franco, D. deMontigny, S. Kentish, J. Perera and G. Stevens, "A Study of the Mass Transfer of CO_2 through Different Membrane Materials in the Membrane Gas Absorption Process," *Sep. Sci. Technol. ,* vol. 43, pp. 225-244, 2008.

[35] M. Mavroudi, S. P. Kaldis and G. P. Sakellaropoulos, "Reduction of CO_2 emissions by a membrane contacting process," *Fuel,* vol. 82, pp. 2153-2159, 2003.

[36] V. Dindore, D. Brilman, F. Geuzebroek and G. Versteeg, "Membrane–solvent selection for CO_2 removal using membrane gas–liquid contactors," *Sep. Purif. Technol.,* vol. 40, no. 2, pp. 133-145, 2004.

[37] S.-H. Lin, C.-F. Hsieh, M.-H. Li and K.-L. Tung, "Determination of mass transfer resistance during absorption of carbon dioxide by mixed absorbents in PVDF and PP membrane contactor," *Desalination,* vol. 249, pp. 647-653, 2009.

[38] Z. Wang, M. Fang, S. Yan, H. Yu, C.-C. Wei and Z. Luo, "Optimization of Blended Amines for CO_2 Absorption in a Hollow-Fiber Membrane Contactor," *Ind. Eng. Chem. Res.,* vol. 52, p. 12170−12182, 2013.

[39] C. Scholes, S. Kentish, G. Stevens and D. deMontigny, "Comparison of thin film composite and microporous membrane contactors for CO_2 absorption into monoethanolamine," *Int. J. Greenhouse Gas Control,* vol. 42, pp. 66-74, 2015.

[40] C. A. Scholes, A. Qader, G. W. Stevens and S. E. Kentish, "Membrane Gas-Solvent Contactor Pilot Plant Trials of CO_2 Absorption from Flue Gas," *Sep. Sci. Technol.,* vol. 49, p. 2449–2458, 2014.

[41] S. Yan, M. Fang, Z. Luo and K. Cen, "Regeneration of CO_2 from CO_2-rich alkanolamines solution by using reduced thickness and vacuum technology: Regeneration feasibility and characteristic of thin-layer solvent," *Chem. Eng. Process.: Process Intensification,* vol. 48, pp. 515-523, 2009.

[42] M. Fang, Z. Wang, S. Yan, Q. Cen and Z. Luo, "CO_2 desorption from rich alkanolamine solution by using membrane vacuum regeneration technology," *Int. J. Greenhouse Gas Control,* vol. 9, pp. 507-521, 2012.

[43] Z. Wang, M. Fang, Q. Ma, Z. Zhao, T. Wang and Z. Luo, "Membrane stripping technology for CO_2 desorption from CO_2-rich absorbents with low energy consumption," *Energy Procedia,* vol. 63, pp. 765-772, 2014.

[44] T. Mulukutla, G. Obuskovic and K. K. Sirkar, "Novel scrubbing system for post-combustion CO_2 capture and recovery: Experimental studies," *J. Membr. Sci.,* vol. 471, pp. 16-26, 2014.